JOURNAL OF CRITICAL REVIEWS

ISSN- 2394-5125 VOL 6, ISSUE 07, 2019

HILL CLIMBING MPPT BASED FAULT RIDE THROUGH CONTROL SYSTEM FOR A WECS WITH DFIG

[1]MR. D.MALLESHAM ASSISTANT PROFESSORMALLESHAMKURUMA@GMAIL.COM

[2]MR. D.MALLESHAM ASSISTANT PROFESSORMALLESHAMKURUMA@GMAIL.COM

[3]MR. VENKATESWAR RAO ASSISTANT PROFESSORVENKATSNMPKMM@GMAIL.COM

DEPARTMENT-EEE

PALLAVI ENGINEERING COLLEGE HYDERABAD, TELANGANA 501505.

Abstract: This paper deals with the Hill climbing MPPT based fault ride-through capability assessment for doubly-fed induction generator-based wind. The most used techniques for MPPT, are the Hill Climbing Techniques. These include Perturb & Observe method and Incremental Conductance. This paper presented an improved fault-ride through (FRT) system for a wind turbine with doubly fed induction generator (DFIG) that is based on the proper HC-MPPT control to address symmetrical as well as unsymmetrical and unbalanced grid voltage sags. This is accomplished by adopting a properly modified topology of the wind energy conversion system (WECS) with DFIG that provides the ability to regulate the stator voltage through the system of the rotor power converters. Therefore, significant improvement of the FRT capability is attained, since any oscillations of both the stator and rotor currents that may be caused by the voltage dip can be considerably reduced and they can remain within predefined safety limits. The implementation of the new topology as well as the corresponding control system are cost effective, since no additional hardware is required, and it is accomplished by the reconfiguration of the existing topology. Simulation results obtained by a high and low scale WECS with DFIG, respectively, are presented to validate the effectiveness of the proposed HC-MPPT and FRT control method and demonstrate the operational improvements

Keywords: Wind Energy Conversion System (WECS), Doubly Fed Induction Generator (DFIG), Hill Climbing (HC) MPPT, Fault Ride Through (FRT)

I.INTRODUCTION

For wind power to take off, however, turbines will need to be built that can both generate power and feed it back into the grid through FRT. Whether or not things return to normal once a voltage drop has been remedied relies on the system's capacity to maintain a steady energy output and avoid excessive current oscillations. However, if a sizable percentage of wind power suddenly ceased operating, it might do major harm to the network [2]. The wind system is very vulnerable to grid disruptions since the stator windings of a DFIG are directly linked to the grid and the rotor side conversion mechanism controls just a portion of the power produced. Given the need of maintaining system function in the face of symmetric and asymmetric network disruptions, the capacity of DFIGs in WECS to perform FRT is of highest value. Large overvoltage and overcurrent transients occur in a DFIG when the rotor moves because the magnetic flux does not immediately adjust to the fast change in stator voltage. A negative sequence component in the stator voltage and a high slip frequency are the results of an asymmetrical breakdown, and they may induce potentially lethal overvoltage and overcurrent oscillations. Several studies have examined the FRT issue in a WECS with DFIG, and the solutions given may be broken down into two groups: hardware interventions and control changes. Most FRT methods include physically restricting the rotor winding connections with a crowbar to protect the rotor side power converters from voltage and current transients [5, 6]. A short circuit is created in the rotor winding due to the resistance of the crowbar. Due to this, the DFIG may wind up resembling an induction machine in appearance. Voltage support is decreased, however, because of the reactive power used by the DFIG to offset large transient stator currents. Regulation of a chopper is demonstrated in [8], where the voltage across a dc link is altered using parallel capacitors; [7] demonstrates an improved version of this technique, known as crowbar control. Using a crowbar in the rotor winding and another in the dc-link, with the latter only activating if the dc-capacitor voltage is over a particular threshold, coordinated crowbar protection [9] may prevent damage to the motor.

ISSN- 2394-5125 VOL 6, ISSUE 07, 2019

The discipline of technical writing has devoted much discussion time to the several strategies for tackling FRTs. Examples of such techniques include superconductor-based systems for current limitation in fault circuits [17-19] and techniques for dynamically restoring voltage in a circuit [10-12]. The stator [13], the rotor [14], and the grid all work together as alternating series voltage compensators to maintain a constant output voltage. In addition, there is a fault current limiter for a saturated core that makes advantage of the difference in permeability between the saturated and unsaturated states and a FRT system that employs series impedance and a rotor crowbar. In we look at the small-signal behaviour and performance of a WECS-DFIG that is wired into a low-voltage, high-impedance ac grid.

It is shown that the low-voltage FRT might be improved by means of a transient reconfiguration control of the power converters in the WECS. In a parallel grid-side rectifier and a series grid-side converter are shown, a hybrid FRT system is shown in action, complete with a switch-type fault current limiter, a brake chopper, and a battery. A FRT method is shown in [12] by presenting a rotor-side converter connected in parallel with a grid-side converter, and the FRT reconfiguration is detailed in detail in [15] by means of a four-switch design with a midway connection. Many hours have been spent contemplating how to improve DFIG regulation of a WECS by increasing the system's FRT capability. In the case of a blackout, a vector hysteresis current regulator PI controller is advised. Using flux-linkage tracking shows how to implement a crowbar-free FRT control strategy for a brushless DFIG running on a supply with voltage dips of equal magnitude everywhere. From the above, one may assume that the suggested FRT solutions that include hardware changes may achieve the FRT goals, but they need additional hardware, which in turn boosts the price of the WECS. However, improving control of FRT might significantly enhance capacity, but the additional complexity of the control system could reduce dependability. Conclusion These findings highlight the necessity for further investigation into the FRT in a WECS equipped with DFIG. A WECS-DFIG that is dependable, low-cost, easy-to-set-up, and capable of handling balanced and unbalanced voltage reductions is required. Several techniques, including as the phase locked loop (PLL), the synchronously rotating reference frame, and the symmetrical component algorithm, have been developed to detect voltage decreases in the grid. The phase shift and grid voltage loss may be mitigated using the voltage harmonic footprint and a matrix technique. Nonlinear adaptive filters, second order generalised integrators, statistical sequential approaches, and the Hilbert-Huang transform are only some of the voltage detection methods documented in the technical literature for the case of WECS with DFIG. The ultimate goal of this study is to advance the state of the art by creating a fault-tolerant WECS-DFIG that can be deployed without substantially increasing the price of installation or the level of complexity of the control system. The proposed system's fault-ride-through capabilities mitigate the production of potentially lethal transient current and voltage in the event of an electrical grid failure. The proposed FRT setup is robust enough to withstand both symmetric and asymmetric voltage drops. During operation of the WECS with DFIG, the stator voltage must be properly adjusted to maintain the nominal value regardless of variations in the grid voltage. So, there's no need for a system to identify problems. As the stator voltage in a rotor power conversion system can be controlled by a grid-side converter. One of the main reasons for developing this control scheme was to improve the efficiency with which DFIG could be used to operate a WECS. To make FRT and DFIG work together in a WECS, we revised the network architecture described. The proposed solution eliminates the transient voltage and current, which are discussed in the technical literature during grid power interruptions and are caused by FRT systems, by directly controlling the stator voltage. This topology relies on a simple rearrangement of the standard WECS architecture, so there is no added time or money needed for its implementation. For the FRT proposal to work, it is assumed that the power factor of the central generator in a wind power system is 1. By changing the WECS-settings, DFIG can function with a variety of power factors. The simulation results account for voltage drops and imbalances on the Grid, both symmetric and asymmetric. This section serves as a quick overview of the paper's key arguments.

ISSN- 2394-5125 VOL 6, ISSUE 07, 2019

III.PROPOSED SYSTEM

TOPOLOGY OF THE FAULT TOLERANT WECS WITH DFIG

The structure of the conventional WECS with DFIG is illustrated in Fig. 1(a). A system of two back-to-back converters at the rotor side are applied, i.e. the generator side converter (GeSC) and the grid side converter (GrSC). A crowbar resistance is utilized to provide FRT capability and a battery storage system (BSS) is employed to smooth the generated electric energy and power. In the conventional topology of Fig. 1(a), The generator side (Gas) device and the grid side (Gs') device are the two components that make up a rotor-side converter pair. Power source and crowbar-based force reduction system Technology to Withstand Physical Attacks (FRT) As can be observed in Figure 1(a), the stator voltage of the DFIG drops dramatically when there are variations in the grid voltage, which has major ramifications for the operating efficiency of the WECS. Adjusting the voltage at the FRT's stator might be one way to make up for the power grid's voltage drop. Because of the malfunction, the voltage and current production have dropped. For instance, the WECS-DFIG design in Fig.1 may be used to accomplish this goal. The secondary windings of the grid transformer are connected to the DFIG stator through a series connection wire. This wire connects the primary windings of the transformer to the electricity grid. The nominal stator voltage of the DFIG may be maintained by the Grosch, depending on the actual grid voltage. Because of this, WECSs with DFIGs may keep running regularly even when transient currents from grid interruptions are present. Figure 6.1 depicts a multi-wound grid transformer, the kind frequently used in a WECS. Only two single-wound transformers are needed to implement the suggested FRT system. Since the rotor and the stator only employ a single winding, the rotor's power rating will be lower. As can be seen in Figure 1, the primary winding of the grid transformer is linked to the secondary winding of the rotor transformer in a DFIG. DFIGs are advantageous because they mechanically separate the stator from the rotor and correctly control the rotor voltage. If the Grosch is handled correctly by the BSS, crowbar resistance in the appropriate control system may not be necessary, and the system may even be fault robust, as shown in Figure 6.1b. The low-pass (LCL) filter in the FRT system is powered by rotor transformer inductances, which are less than those in the other WECS topologies (see Fig.1). Because a simpler LCL filter is employed when the crowbar is not in use, two single-winding transformers may be utilised instead of the more expensive multi-winding transformer shown in Fig.1, resulting in a cost reduction. No increase in WECS cost is anticipated as a consequence of implementing FRT.

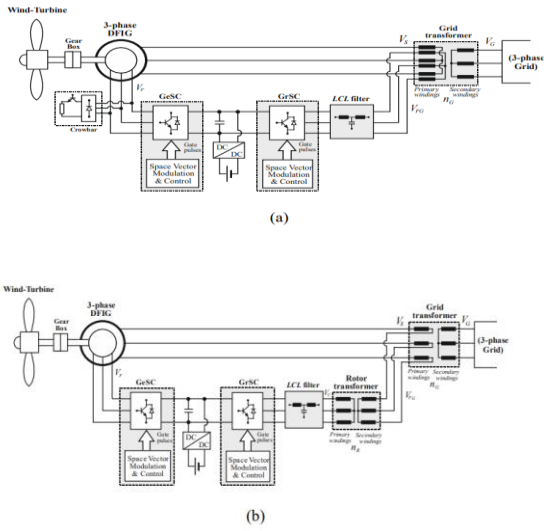

Fig.1. Comparison of the structure of a variable speed WECS with DFIG: (a) conventional and (b) improved FRT capability system.

A dc-dc converter and battery storage system are essential components of any reliable power management scheme (BSS). The BSS in the WECS design shown in Fig. 1(b) is responsible for maintaining a stable dc-link voltage, which is crucial for maximising the effectiveness of the FRT control. This is done in line with the power capacity and the building of the power equipment, two of the most important aspects in determining the total cost of a WECS. As a result of using cheaper alternatives, the typical WECS DFIG's FRT configuration has changed. Figure 1(b) depicts the topological modifications we made to the

ISSN- 2394-5125 VOL 6, ISSUE 07, 2019

WECS for fault tolerance so that it would cost as little as a regular system. Cost estimates are presently difficult to provide owing to factors such as the fluctuating cost of equipment and the specific technical components of the wind system. Clearly, the suggested FRT design in Fig.1(b) has higher power losses and worse system efficiency than the grid transformer in Fig. 1(a) due to the additional iron loss in the core of the rotor transformer (a). Since the rotor transformer operates at a lower voltage, its additional iron loss (shown in Figure 1(b)) is less than the grid transformer's. The LCL filter shown in Fig. 1(b) offers many advantages over the LCL filter shown in the normal WECS in Fig.1, including reduced iron and copper losses, fewer windings, and a higher working voltage. This shows that when a WECS is constructed with a DFIG utilising the proposed FRT structure, system efficiency is not dramatically impacted.

FRT CONTROL IN A WECS WITH DFIG

Positioning the stator flux-linkage along the d-axis (s= ds) allows for decoupling control in a DFIG.

$$\psi_{qs} = 0 \tag{1}$$

Considering that

$$\psi_{qs} = L_{ls} I_{qs} + L_m (I_{qs} + I_{qr}) \tag{2}$$

Results

$$I_{qr} = -\frac{L_m + L_{ls}}{L_m} I_{qs} \tag{3}$$

square and ds are the q- and d-axis components of the stator flux-linkage, whereas Lom and LLCs are the magnetising and stator leakage inductances, respectively. The reactive power at the stator of a DFIG may be determined using the formula

$$Q_s = 1.5(I_{ds} V_{qs} - I_{qs} V_{ds}) \tag{4}$$

Were

$$V_{qs} = R_s I_{qs} + \omega_e \psi_{ds} \tag{5}$$

$$V_{ds} = R_s I_{ds} + \omega_e \psi_{qs} \tag{6}$$

are the q- and d-axis components of the DFIG stator voltage Vs. In light of (1), we are able to

$$Q_s = 1.5 I_{ds} \psi_{ds} \omega_e \tag{7}$$

As shown in Fig. 1, the primary windings of the grid transformer serve as the geographic CenterPoint of the series connection between the DFIG stator and the secondary windings of the rotor transformer (a). The DFIG stator runs with zero reactive power (Q s=0) to obtain a power factor of one at the point of common connection to the grid. The DFIG uses gas since it is the only rotor-side reactive power source. The Grosch provides reactive power to the grid transformers and DFIG rotor. Given our current understanding and the fact that ds cannot equal zero, we may infer that

$$I_{ds} = 0 \tag{8}$$

By using (1) and (8) in (6), yields

$$V_{ds} = 0 \tag{9}$$

Considering that

$$\psi_{ds} = L_{ls} I_{ds} + L_m (I_{ds} + I_{dr}) \tag{10}$$

and due to (8), results

$$\psi_{ds} = L_m I_{dr} \tag{11}$$

Accordingly, the d-axis component of the current in a DFIG's rotor can be expressed as

ISSN- 2394-5125 VOL 6, ISSUE 07, 2019

$$I_{dr} = \frac{V_{qs} - R_s I_{qs}}{\omega_e L_m} \quad (12)$$

air-gap flux-linkage thus

$$\psi_m = L_m I_{dr} \quad (13)$$

In order to calculate the VoVo of the Grass's output, we use (14), since the power factor at the point of common coupling to the grid is 1.

$$V_{qCov} = n_R \left(V_{qs} - n_G V_{Gq} - I_{qs} R_{Tr} \right) \quad (14)$$

$$V_{dCov} = \omega_e L_{Tr} I_{qs} \quad (15)$$

Find the low-pass filter and rotor transformer's equivalent inductance.

When the grid voltage drops, the DFIG keeps normal operation going by keeping the stator voltage at its nominal value, which keeps the rotor and stator currents within safe operating limits. This implies that the Vs. must be maintained at the same level as the stator's nominal voltage, as shown in. You can modify the Grass's output voltage, for example.

$$V_{qCov} = n_R \left(V_{s\_nom} - n_G V_{Gq} - I_{qs} R_{Tr} \right) \quad (16)$$

Regardless of changes in the VG grid voltage, Vs. is kept at Vs nom thanks to the precise control offered by VoVo (16). The WECS-DFIG control system is shown in Fig. 2, and it is fault tolerant. The Grosch has to communicate with the d and q axis controls of the FRT for precise Vidicon and Vicon calculations. Currently (15), (16). In (12), we see that the DFIG's excitation field controller is responsible for supplying the Dir current, while the MPPT controller uses the HC-MPPT computation to regulate the Ire current. The in-charge Gas regulator thinks about all these factors. Without a fault detection system, the suggested FRT technique may be implemented by vigilant monitoring of the grid voltage (VG) and adjustments to the VoVo according to the formula (16). The second-harmonic interference induced by the grid voltage's d-q transformation may be mitigated with the use of a low pass filter (LPF) that monitors the q-axis of the grid voltage. The turn ratio of the rotor transformer is independent of the voltage on the WECS rotor side. The rotor side charges the batteries and feeds extra energy into the grid while the DFIG is working at super-synchronous speed, its most efficient setting. Batteries are used to power the DFIG's rotor when the wind is too feeble to keep the generator operating in synchronous mode. However, the DFIG configuration will dictate how the battery's power is distributed. The DFIG's rotor and grid are driven by a negative current during sub-synchronous operation, whereas a positive current is used for super-synchronous operation. As the DFIG operates in a sub-synchronous mode, nominal power generated by the WECS is lost very little in the low wind speed sector. The fault tolerant WECS with DFIG cannot operate without a BSS that has a limited energy capacity. When the BSS's stored energy isn't enough to power the DFIG, it may pull the necessary electric energy from the grid through the Grosch, reducing the VoVo and/or the Ire to limit the DFIG's rotor side energy demands during prolonged periods of low wind speed. The appropriate size of the battery stack can only be determined by taking into account the energy storage needs for delivering adequate power and energy smoothing, as well as the energy requirements at low wind speed to maintain a stable dc-link voltage. The cost of the battery system has to be considered with the financial objectives of the WECS. Therefore, a techno-economic evaluation that factors in the aforementioned criteria and the wind potential of the area where the WECS will be installed should be used to calculate the appropriate nominal energy capacity of the BSS. The suggested FRT control system might be used with few changes by a wide variety of DFIG wind turbines over a wide power range. East (15), (16), and (12) for the Maximum Power Point Tracking (MPPT) controller; and west. New controller implementation strategies and more subtle parameter choices may improve maximum power point tracking (MPPT) in high-power devices. Any wind turbine using DFIGs may benefit from the FRT control technique and WECS-DFIG architecture shown in Fig.2

ISSN- 2394-5125 VOL 6, ISSUE 07, 2019

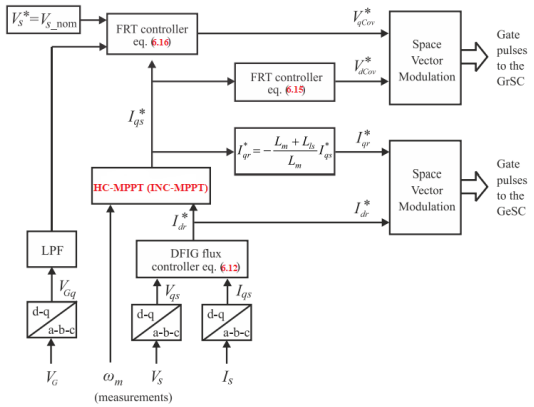

Fig. 2. Proposed FRT control strategy for a WECS with DFIG

III. HILL CLIMBING MPPT

A power metre is all that's required to implement HCS, making it a very simple MPPT method. Evidence linking the shaft speed of a turbine to its mechanical output inspired this concept. There is flexibility in how HCS systems are implemented, since they may use either a constant or variable step size, or even two distinct step sizes working in tandem.

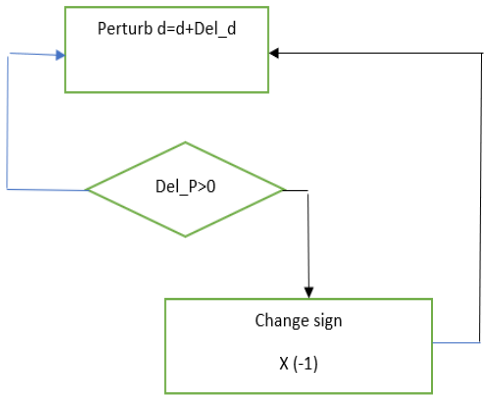

Fig. 3: Principle of HCS

III.SIMULATION RESULTS

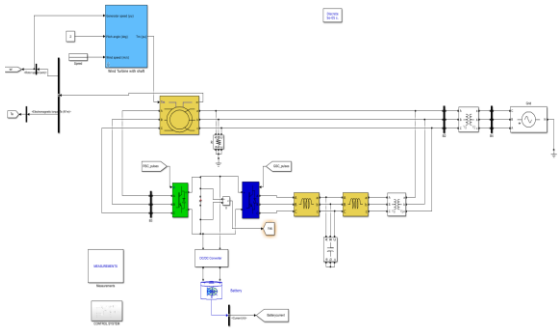

Fig .4 MATLAB/SIMULINK circuit diagram of the system

A) EXISTING RESULTS

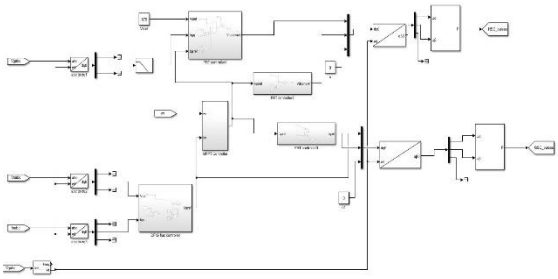

Fig.5 Existing FRT control strategy for a WECS with DFIG

Figures.6 and 7 show the WECS in action during low wind speeds (represented by a symmetrical grid voltage disturbance from 100% to 20% and then 100% of the nominal value) and high wind speeds. Changes in the stator voltage's THD% are depicted in Fig.8 when the grid voltage varies from 100% to 20% of the nominal value, as depicted in Fig 9.

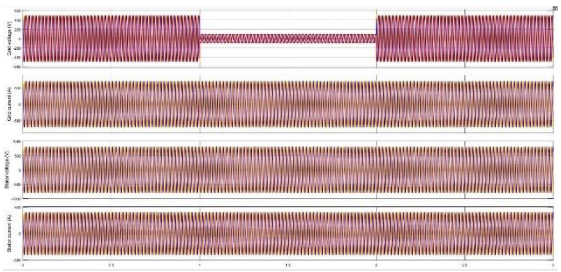

ISSN- 2394-5125 VOL 6, ISSUE 07, 2019

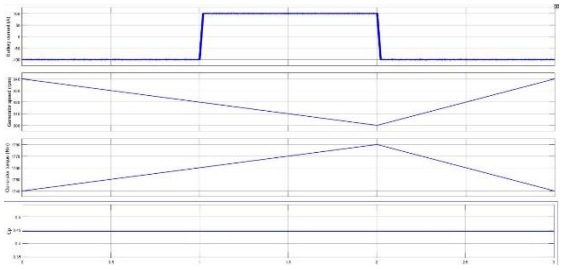

Figure.6 depicts the results of a simulation run on the proposed FRT wind system with a DFIG of 1.6 MW in light wind (4.5 m/s) and a symmetrical grid voltage disturbance (100% to 20% and back to 100% of the nominal value).

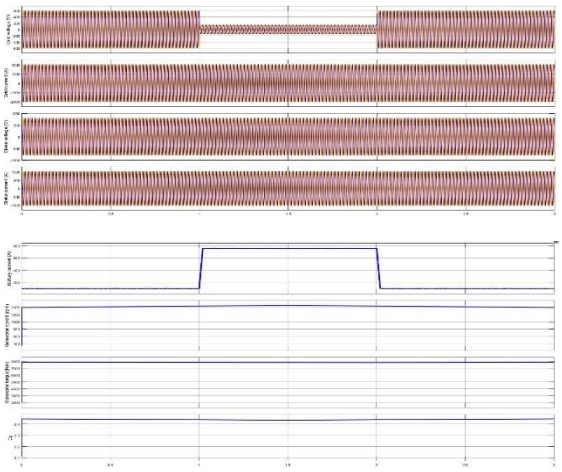

Figure.7 shows the proposed FRT wind system with DFIG of 1.6 MW performs well in simulations run under high wind conditions (9 m/s) and a symmetrical grid voltage disturbance (100% to 20% and back to 100% of the nominal value).

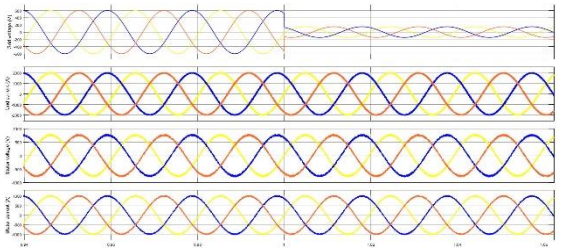

Fig.8 Simulation results (WECS with DFIG of 1.6-MW) during the time the grid voltage disturbance from 100% to 20% of the nominal value occurs (wind speed 9 m/s).

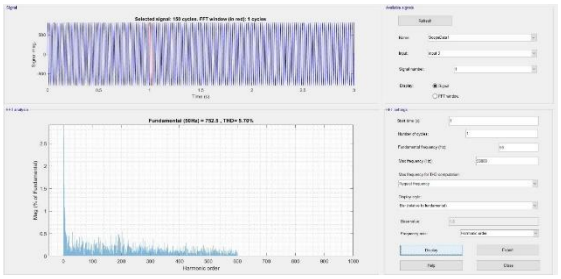

Fig.9 THD% of stator voltage is 5.70%

B) EXTENSION RESULTS

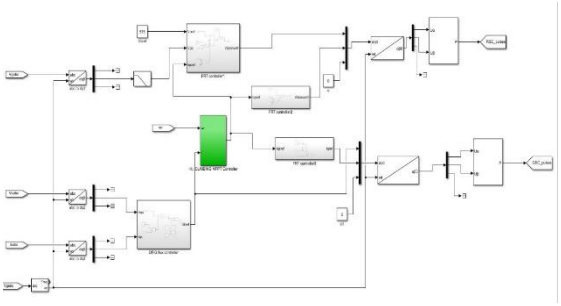

Fig.10 Proposed FRT control strategy for a WECS with DFIG

Figures.11 and 12 depict the low and high wind speed results of the WECS under a symmetrical grid voltage disturbance of 100% to 20% and back to 100% of the normal value. Figure 13 demonstrates a decrease in the THD% of the stator voltage relative to the existing arrangement.

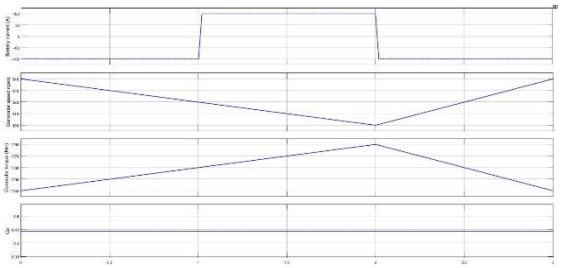

Figure.11 Simulation results of proposed FRT wind system with a DFIG of 1.6 MW under symmetrical grid voltage disturbance (100% to 20% and back to 100% of the nominal value) and low wind circumstances (4.5 m/s).

ISSN- 2394-5125 VOL 6, ISSUE 07, 2019

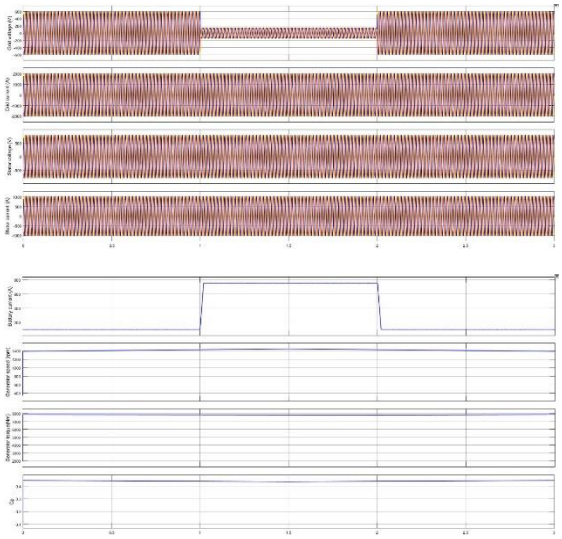

Figure.12 A simulation of the proposed FRT wind system with DFIG of 1.6 MW which was run with a grid voltage disturbance of 100%, 20%, and 100% of the nominal value, and a wind speed of 9 m/s.

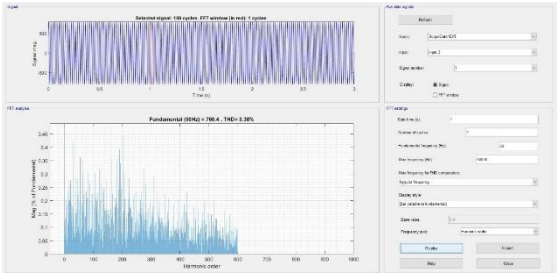

Fig.13 THD% of stator voltage is 3.38%

COMPARISION TABLE

	Existing system	**Extension system**
Stator current THD%	5.70%	3.38%

CONCLUSION

A HC-MMPT based FRT control system for a WECS with DFIG has been proposed in this paper. A new WECS topology has been adopted that gives the ability to control the stator of the DFIG. Specifically, by properly controlling the rotor side converter of the DFIG, the stator voltage can be kept constant at the nominal value and thus, a fault diagnosis system is not required. Therefore, the WECS can continue the operation without being affected by any symmetrical, unsymmetrical, and unbalanced grid voltage disturbances, and thus, no transient current and voltages are caused. The implementation of the proposed FRT control system does increase the cost of WECS compared to the conventional system, since it is based on the proper modification by replacing expensive components of the conventional system with low cost components and vice versa. The effectiveness and the high performance of the proposed HC-MPPT based FRT control scheme have been validated with several simulation results obtained by a high power WECS-DFIG of 1.6-MW. The proposed system gives less THD compared to existing system.

REFERENCES

[1] E. Hau, Wind Turbines: Fundamentals, Technologies, Application, Economics, Springer-Verlag: 2013, 3rd Edition.

[2] A. El-Naggar and I. Erlich, 'Fault current contribution analysis of doubly fed induction generator-based wind turbines', IEEE Trans. Energy Conv., vol. 30, no. 3, pp. 874-882, Sept. 2015.

[3] D. Xiang, L. Ran, P.J. Tanner, and S. Yang, 'Control of a doubly fed induction generator in a wind turbine during grid fault ride-through', IEEE Trans. Energy Conv., vol. 21, no. 3, pp. 652-662, Sep. 2006.

[4] S. Seman, J. Niiranen, and A. Arkie, 'Ride-through analysis of doubly fed induction wind-power generator under unsymmetrical network disturbance', IEEE Trans. Power Syst., vol. 21, no. 4, pp. 1782–1789, Nov. 2006.

[5] J. Morren and S.W.H. de Haan, 'Ride through of wind turbines with doubly-fed induction generator during a voltage dip', IEEE Trans. Energy Conv., vol. 20, no. 2, pp. 435-441, June 2005.

[6] L.G. Megajoule, T. Littler, and D. Flynn, 'Decoupled-DFIG fault ride-through strategy for

ISSN- 2394-5125 VOL 6, ISSUE 07, 2019

enhanced stability performance during grid faults', IEEE Trans. Sustain. Energy, vol. 1, no. 3, pp. 152-162, Oct. 2010.

[7] F.K.A. Lime, A. Luna, P. Rodriguez, E.H. Watanabe, and F. Blaabjerg, 'Rotor voltage dynamics in the doubly fed induction generator during grid faults', IEEE Trans. Power Electron., vol. 25, no. 1, pp. 118-130, Jan. 2010.

[8] L. Huchel, M.S. El Morsi, and H.H. Seinfeldian, 'A parallel capacitor control strategy for enhanced FRT capability of DFIG', IEEE Trans. Sustain. Energy, vol. 6, no. 2, pp. 303-312, April 2015.

[9] A.M.A. Haidar, K.M. Muttaqi, and M. Tarafdar, 'A coordinated control approach for DC link Nd roto crowbars to improve fault ride-through of DFIG-based wind turbine', IEEE Trans. Ind. Appl., vol. 53, no. 4, pp. 4073-4086, July/Aug. 2017.

[10] C. Wessels, F. Gebhardt, F.W. Fuchs, 'Fault ride-through of a DFIG wind turbine using a dynamic voltage restorer during symmetrical and asymmetrical grid faults', IEEE Trans. Power Electron., vol. 26, no. 3, pp. 807-814, March 2011.

[11] A.O. Ibrahim, T.H. Nguyen, D.C. Lee, and S.C. Kim, 'A fault ride through technique of DFIG wind turbine systems using dynamic voltage restorers', IEEE Trans. Energy Conv., vol. 26, no. 3, pp. 871-881, Sept. 2011.

[12] R.A. Amador payara, P. Kalian nan, S. Padmanaban, U. Subramaniam, and V.K. Ramachandra Murthy, 'Improved fault ride through capability in DFIG based wind turbines using dynamic voltage restorer with combined feed-forward and feed-back control', IEEE Access, vol. 5, no. 20494-20503, Oct. 2017.

[13] S. Zhang, K.J. Tseng, S.S. Choi, T.D. Nguyen, and D.L. Yao, 'Advanced control of series voltage compensation to enhance wind turbine ride through', IEEE Trans. Power Electron., vol. 27, no. 2, pp. 763-772, Feb. 2012.

[14] J. Mohammadi, S. Afshar Nia, S. Vaez-Zadeh, and S. Firangi, 'Improved fault ride through strategy for doubly fed induction generator-based wind turbines under both symmetrical and asymmetrical grid faults', IET Renew. Power Gener., vol. 10, no. 8, pp. 1114-1122, June 2016.

[15] P.H. Huang, M.S. El Morsi, S.A. Hasen, 'Novel fault ride-through scheme and control strategy for doubly fed induction generator-based wind turbine', IEEE Trans. Energy Conv., vol. 30, no. 2, pp. 635-645, June 2015.

[16] P.H. Huang, M. Shawky, W. Xiao, and J.L. Kirtley Jr., 'Novel fault ride through configuration and transient management scheme for doubly fed induction generator', IEEE Trans. Energy Conv., vol. 28, no. 1, pp. 86- 94, March 2013.

[17] M. Elsheikh, D.E.A. Mansour, and A.M. Azmy, 'Improving fault ride through capability of DFIG-based wind turbine using superconducting fault current limiter', IEEE Trans. Applied Superconductivity, vol. 23, no. 3, June 2013.

[18] L. Chen, C. Deng, F. Zheng, S. Yi, Y. Liu, and Y. Liao, 'Fault ride through capability enhancement of DFIG-based wind turbine with a flux-coupling-type SFCL employed at different locations', IEEE Trans. Appl. Superconductivity, vol. 25, no. 3, pp. 5201505, June 2015.